Electronic Supplementary Information

Enhancement of the catalytic activity of Mg/Al layered double hydroxide for glycerol oligomers production

Fernando J. S. Barros[a], Yue Liu[b], Clarissa D. Paula [a],Francisco Murilo T. de Luna[a], Enrique Rodríguez-Castellón[c], Rodrigo S. Vieira[a*]

[a.]Universidade Federal do Ceará, Departamento de Engenharia Química, Grupo de Pesquisa em Separações por Adsorção – GPSA, Campus do Pici, 709, Fortaleza, CE, 60.455-760, Brazil . E-mail: rodrigo@gpsa.ufc.br

[b.]Department of Chemistry and Catalysis Research Center, TU München, Garching 85748, Germany.

[c.]Facultad de Ciencias, Departamento de Química Inorgánica, Mineralogía y Cristalografía (Unidad Asociada ICP-CSIC), Universidad de Málaga, Campus de Teatinos s/n, 29071 Malaga, Spain.

Table S1 Thermogravimetric analysis of MAS, MAC, MAU05, MAU1, MAM1 and MAM24.

Sample	W_1 (%)	W_2 (%)	W_{Total} (%)
MAS	13.93	30.75	44.68
MAC	9.95	18.83	28.78
MAU05	11.26	32.61	43.87
MAU1	12.49	31.71	44.2
MAM1	11.04	31.64	42.68
MAM24	14.8	30.94	45.74

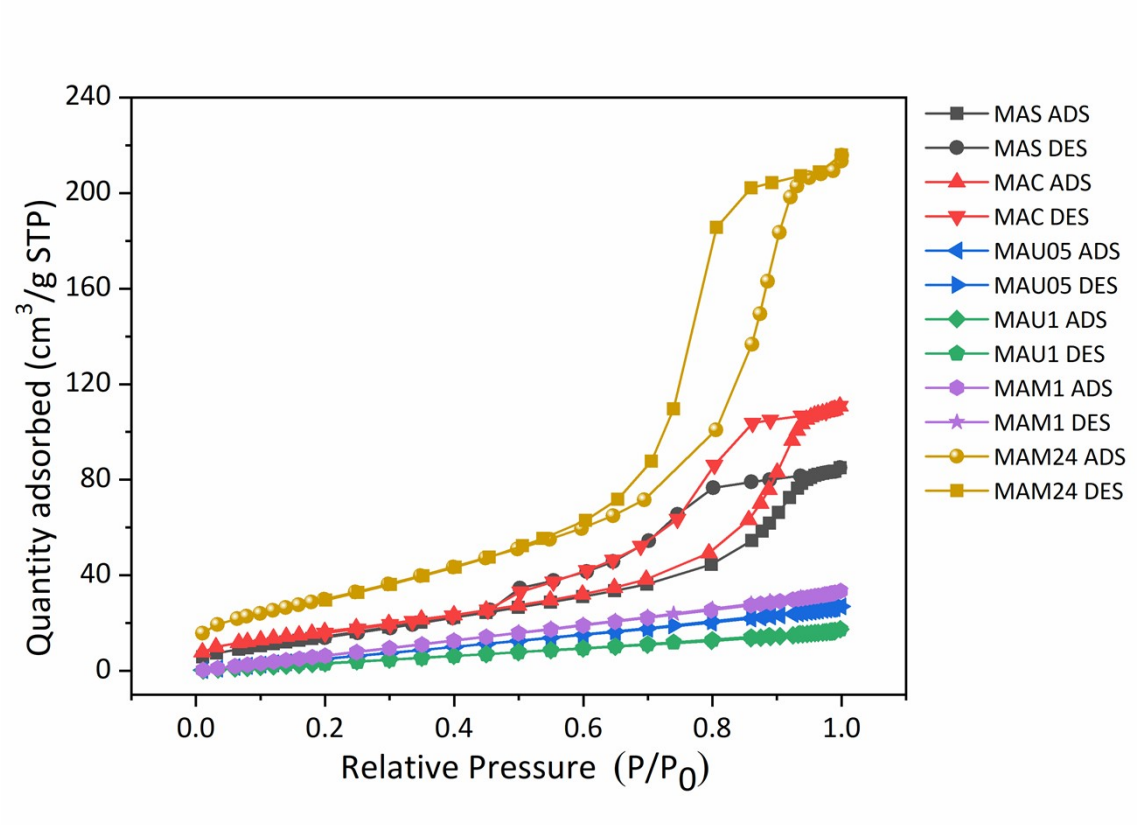

Fig.S1 N_2 isotherms for MAS, MAC, MAU05, MAU1, MAM1 and MAM24.

The N_2 adsorption isotherms of MAS, MAC and MAM24 resembles type IV isotherm, with the presence of a hysteresis loop (type H2b) caused by capillary condensation, indicating the mesoporous nature of the catalysts with relatively lower specific surface area [1]. MAU05, MAU1 and MAM1 isotherms resembles type II, the differences on the initial part of the isotherm can be due to operational reasons.

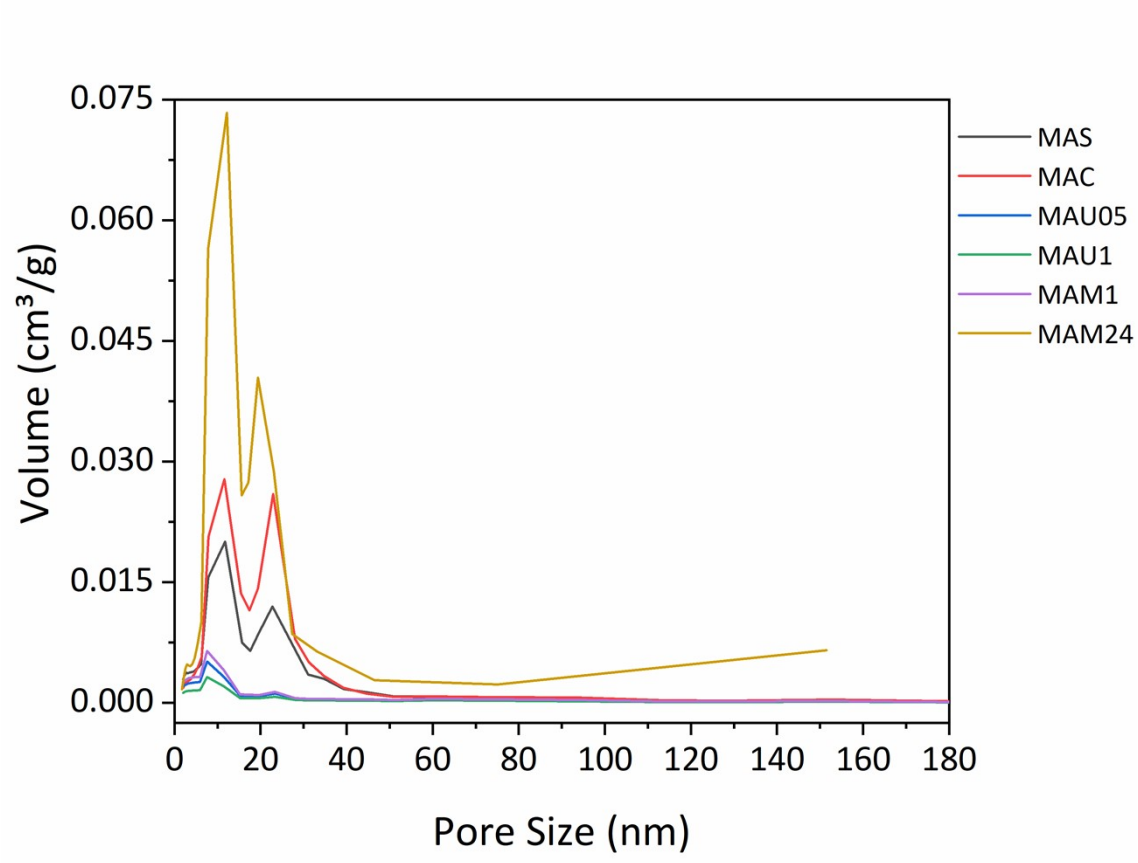

Fig. S2 BJH pore size distribution for MAS, MAC, MAU05, MAU1, MAM1 and MAM24.

Mesoporous character of all samples was confirmed by its pore size distribution in Fig. S2 (ESI†), MAM24 was the only one to present similar D_p to MAS and MAC, in agreement with the increasing on the other textural properties.

(a)

(b)

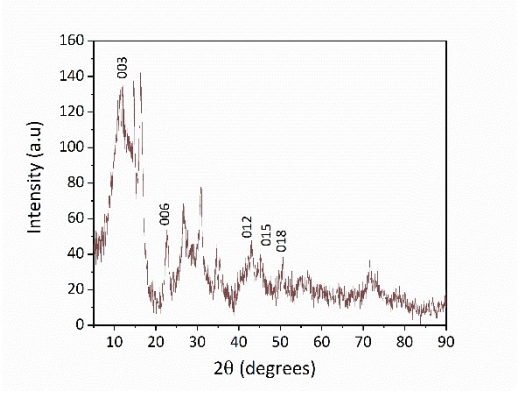

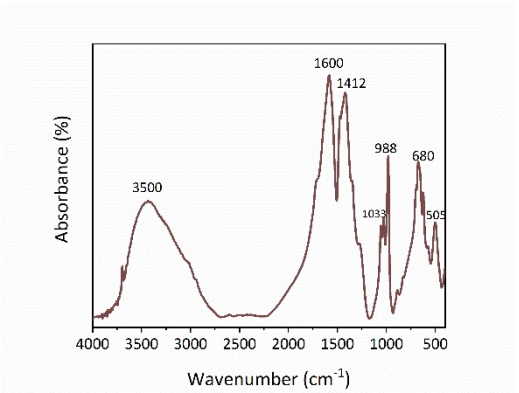

(c)

(d)

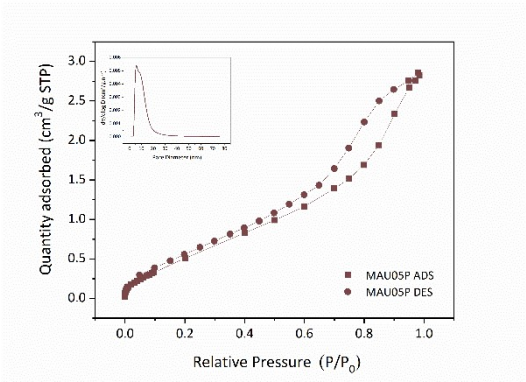

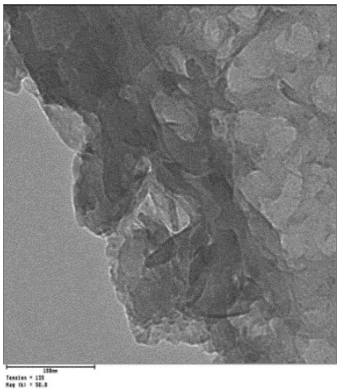

(e)

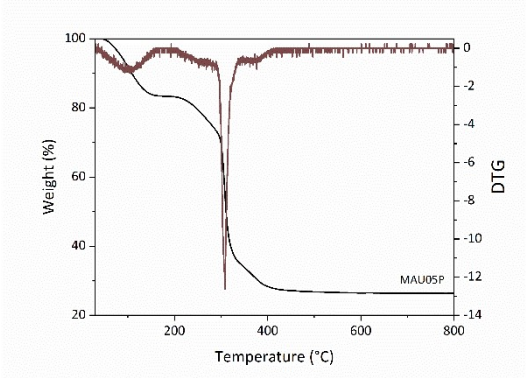

Fig.S3 MAU05P characterizations: a) XRD, b) FTIR, c) N_2 isotherm and pore size distribution, d) TEM (0.1 µm) and e) TGA/DTG.

The addition of acetic acid led to a material with the same diffractogram peaks of MAU05, Fig. S3a). However, the increase of noise points to a lower crystallinity. Regarding FTIR, Fig. S3b), the main difference in comparison with MAU05 is the presence of bands characteristic of acetic acid from 1300 to 500 cm^{-1}, indicating that some amount of acid remains after drying. Figure S3c) shows the nitrogen isotherm, before the addition of acetic acid material was type II and after that became type IV, suggesting the appearance of mesoporosity. Textural properties have changed, S_{BET} dropped from 44 to 24 m^2g^{-1}, V_P went from 0.04 to 0.05 cm^3 g^{-1} and D_P increased from 3.33 to 7.58 nm. Pore size distribution highlights this change of D_p.TEM image, Fig. S3d), suggests that morphology was not affected by the addition of acetic acid, since characteristic agglomerates of platelets are still present. TGA is presented in Fig. S3e), values of weight loss for this material are 16.9% for the first step (adsorbed water) and 56.68% for the second, compared to 11.3% and 32.61% for MAU05, respectively. Such behavior must be related to the presence of remaining acetic acid.

(a)

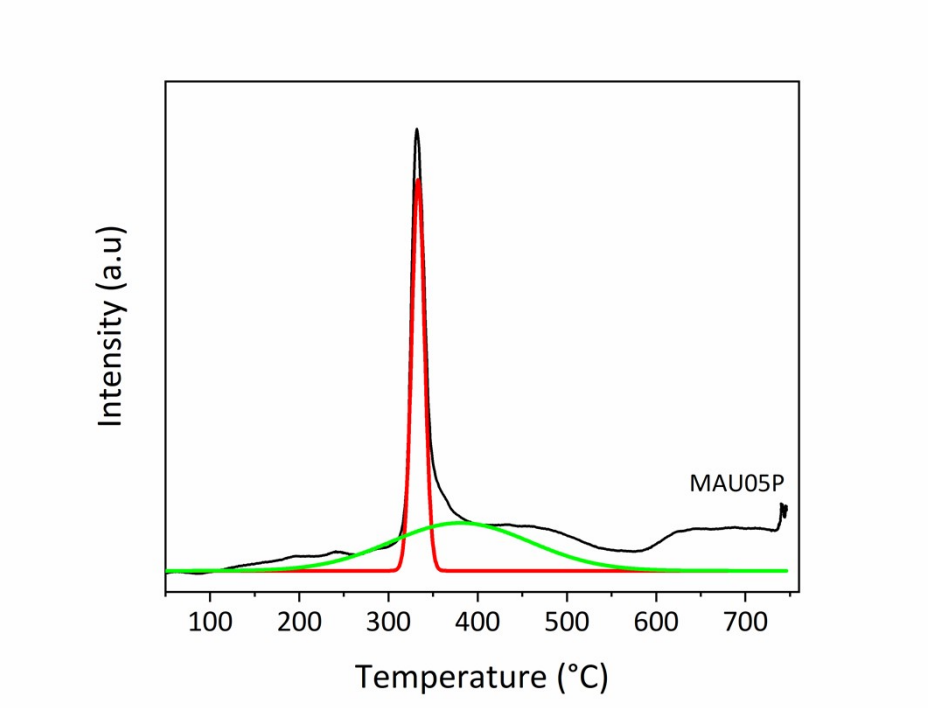

(b)

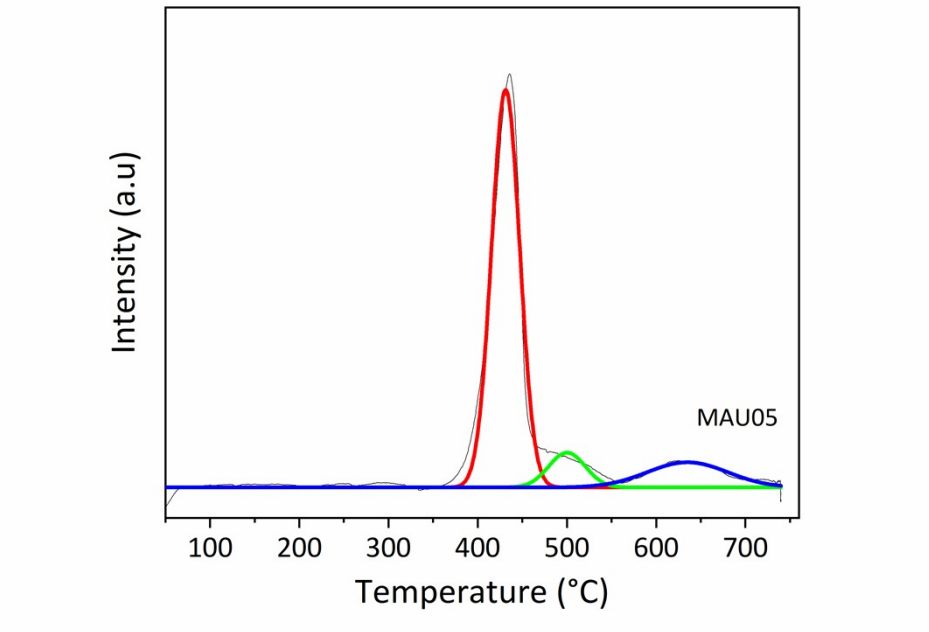

Fig. S4 CO_2-TPD profiles for a) MAU05P and b) MAU05.

Table S2 Selectivity to acrolein for reactions with MAC and rehydrated catalysts.

Test	Sample	S_{Acr} (%)
Reaction Temperature	210 °C	0.42
(4 wt% MAC and 24 hours)	220 °C	0.17
	230 °C	0.07
	240 °C	0.15
MAC Loading	2%	0.15
(240 °C and 24 h)	3%	0.02
	4%	0.15
Reaction time	8 h	0.11
(4 wt% MAC and 240 °C)	24 h	0.13
Rehydrated LDH	MAC	0.11
(4 wt%, 240 °C and 8 h)	MAU05	0.11
	MAU1	0.06
	MAM1	0.12
	MAM24	0.06

Test	Sample	SAcr (%)
MAU05	1st run	0.03
(4%wt, 240 °C and 8 h)	2nd run	0.29
	3rd run	0.25
	4th run	1.82

Table S3 Selectivity to acrolein for the reusability test of MAU05.

Test		Mg (ppm)	Al (ppm)
Glycerol (reactant)		-	-
MAU05	1st run	-	-
(4%wt, 240 °C and 8 h)	2nd run	-	-
	3rd run	-	-
	4th run	-	-
CD[12]	1st run	160	N.A
(2%wt, 220 °C and 24 h)	2nd run	190	N.A
	3rd run	240	N.A

Table S4 ICP results for reusability tests of MAU05 and calcined dolomite (CD)[2].

N.D Non applicable

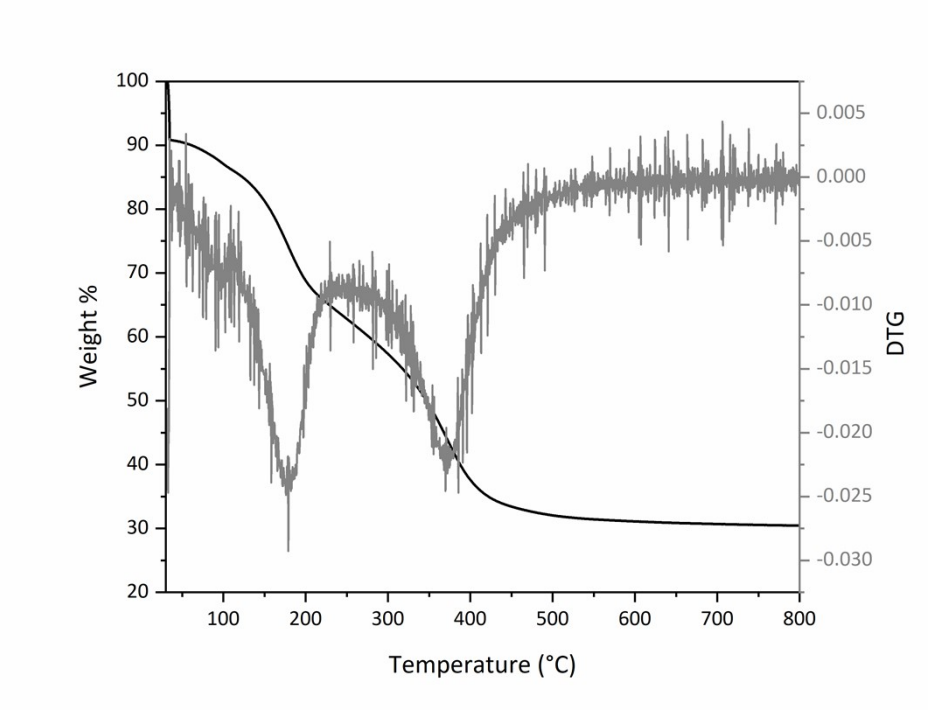

Fig. S5 TGA/DTG for MAU05 spent catalyst after the 3rd reaction cycle (reactions conditions: 4 wt% cat., 240 °C and 8 h).

(a)

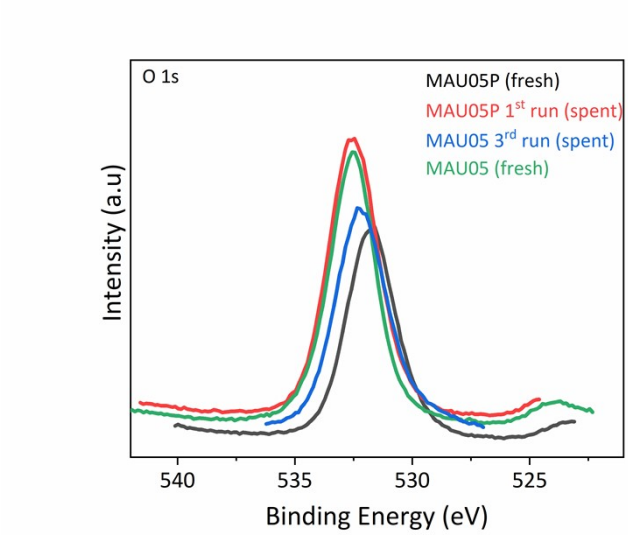
O 1s
MAU05P (fresh)
MAU05P 1st run (spent)
MAU05 3rd run (spent)
MAU05 (fresh)
Intensity (a.u)
540
535
530
525
Binding Energy (eV)

(b)

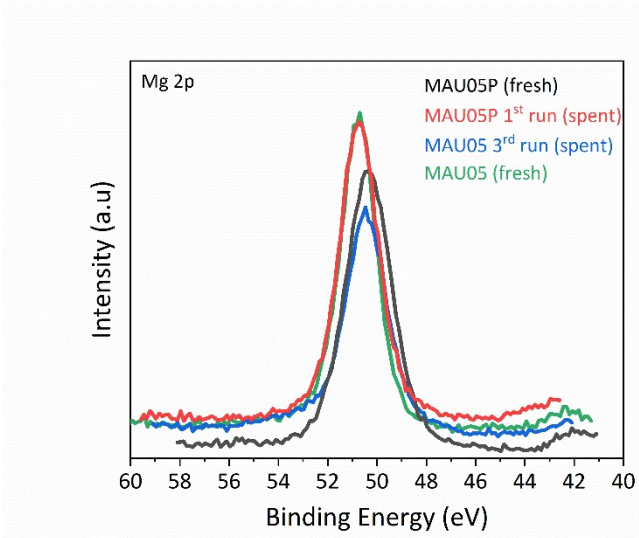
Mg 2p
MAU05P (fresh)
MAU05P 1st run (spent)
MAU05 3rd run (spent)
MAU05 (fresh)
Intensity (a.u)
60
58
56
54
52
50
48
46
44
42
40
Binding Energy (eV)

(c)

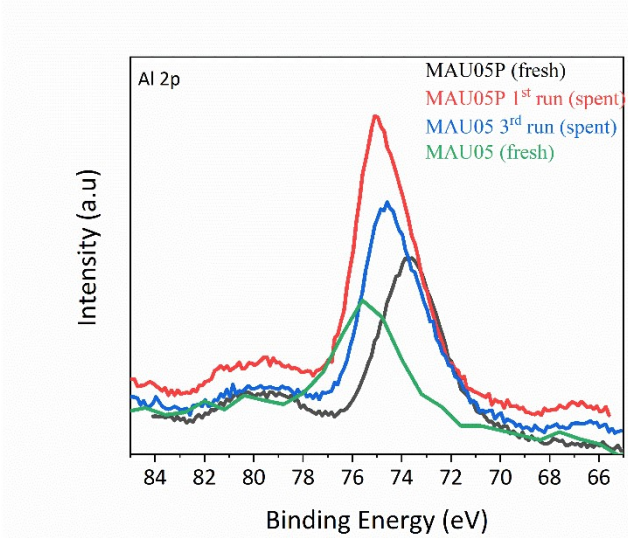
Al 2p
MAU05P (fresh)
MAU05P 1st run (spent)
MAU05 3rd run (spent)
MAU05 (fresh)
Intensity (a.u)
84
82
80
78
76
74
72
70
68
66
Binding Energy (eV)

Fig. S5 XPS spectra for fresh and spent MAU05 and MAU05P: a) O 1s, b) Mg 2p and c) Al 2p regions.

The comparison of the spectra of MAU05 and MA05P in fresh forms showed that the intensity of Mg 2*p* signal decreased and, conversely, that of Al 2*p* increased with the addition of acetic acid. As discussed in the manuscript, there is a surface enrichment of Al.

Regarding the Mg 2*p* region, in all samples there is a single contribution ranging from 50.4 to 50.7 eV. For the Al 2*p* signal, the binding energy values are from 73.3 to 75 eV. Both results are related to the hydroxide form, these findings are supported by the O 1s core level spectra. [3]

For the O 1*s* signal, MAU05 displays a band at around 532.5 eV, related to the hydroxide form. After three reaction cycles, the signal can be deconvoluted into two contributions, the main contribution has the binding energy reduced to 532.2 eV and the second at 530 eV, attributed to the presence of O^{2-}. [3,4] MAU05P presents a single band at around 531.7 eV, related to the carbonate group. Conversely, the recovered spent catalyst from the first run has this band shifted to 532.5 eV, indicating compositional change from carbonate to hydroxide

REFERENCES

1 H. Mitta, P. K. Seelam, K. V. R. Chary, S. Mutyala, R. Boddula and A. M. Asiri, *Glob. Challanges*, 2018, **2**, 1–12.

2 F. J. S. Barros, J. A. Cecilia, R. Moreno-Tost, M. F. de Oliveira, E. Rodríguez-Castellón, F. M. T. Luna and R. S. Vieira, *Waste and Biomass Valorization*, 2018, **0**, 1–14.

3 A. H. Padmasri, A. Venugopal, V. D. Kumari, K. S. R. Rao and P. K. Rao, *J. Mol. Catal. A Chem.*, 2002, **188**, 255–265.

4 P. Guerrero-Urbaneja, C. García-Sancho, R. Moreno-Tost, J. Mérida-Robles, J. Santamaría-González, A. Jiménez-López and P. Maireles-Torres, *Appl. Catal. A Gen.*, 2014, **470**, 199–207.